

Growth Factors, Cytokines, Cell Cycle Molecules

# The Novel Cytokine p43 Stimulates Dermal Fibroblast Proliferation and Wound Repair

Sang Gyu Park,\* Hyosook Shin,\*  
Young Kee Shin,\* Yeonsook Lee,†  
Eung-Chil Choi,\* Bum-Joon Park,\* and  
Sunghoon Kim\*

From the National Creative Research Initiatives Center for Aminoacyl-tRNA Synthetase (ARS) Network,\* College of Pharmacy, and Imagen Company Biotechnology Incubation Center,† Seoul National University, Seoul, Korea

**The multifunctional cytokine p43 acts on endothelial and immune cells to control angiogenesis and inflammation. In this report, we describe an additional activity of p43 that specifically promotes fibroblast proliferation and wound repair. In skin wound regions from mice, tumor necrosis factor- $\alpha$  induced p43 expression and secretion from macrophages recruited to the site. p43 also promoted fibroblast proliferation through its 146-amino acid N-terminal domain as revealed by deletion mapping. This p43-induced fibroblast proliferation was mediated by extracellular signal-regulated kinase (Erk). Depletion of endogenous p43 in mice by gene disruption retarded wound repair, whereas exogenous supplementation of recombinant human p43 to the wound area stimulated dermal fibroblast proliferation, collagen production, and wound closure. Thus, we have identified a novel p43 activity involving the stimulation of fibroblast proliferation, which could be applied therapeutically to aid wound repair. (Am J Pathol 2005, 166:387–398)**

Because skin is the first defensive system, efficient healing of cutaneous injuries is important to prevent infection by foreign pathogens.<sup>1</sup> Skin injuries recover through a multistage process including coagulation, inflammation, proliferation, and tissue remodeling, each of which is achieved via the complex interplay of diverse growth factors, cytokines, and cell cycle regulators.<sup>2</sup> Here we report that p43 can promote the skin repair process by boosting the proliferation of dermal fibroblasts.

Although p43 was first identified as a factor associated with a macromolecular protein complex consisting of several different aminoacyl-tRNA synthetases,<sup>3,4</sup> it is also

secreted from different types of cells, including prostate cancer,<sup>5</sup> immune, and transfected cells.<sup>6</sup> The secreted p43 activates monocytes/macrophages to induce various proinflammatory cytokines, such as tumor necrosis factor (TNF)- $\alpha$  and interleukin-8,<sup>6–8</sup> and also controls angiogenesis by a dual mechanism involving the migration and death of endothelial cells.<sup>9</sup> Because inflammation and angiogenesis constitute important parts of the wound-healing process,<sup>1,10</sup> we expected that p43 may play a role in the wound repair process. To evaluate the significance of p43 in this process, we set up a cutaneous wound model in mice, and examined the behavior and activity of p43 in the wound region. From various analyses using cell and animal models, we found a new activity of p43 in the proliferation of fibroblasts and wound repair. This activity was specific to fibroblasts, and distinct from its effects on monocytes/macrophages and endothelial cells that we previously reported. The exogenous supplementation of p43 promoted the wound-healing process through the enhanced proliferation of fibroblasts and the deposition of collagen, and conversely, the targeted disruption of the p43 gene in mice retarded the wound closure, proving its functional significance in dermal fibroblast proliferation and wound repair. The results obtained in this work led us to propose that p43 is a novel signaling factor involved in the dermal fibroblast proliferation required for wound repair.

## Materials and Methods

### Skin Wound Generation and Histological Analyses

For the *in vivo* wound experiments, we used 8-week-old male C57BL/6 mice (p43<sup>+/+</sup> and p43<sup>-/-</sup>). We anesthetized the mice with an intraperitoneal injection of 2.5%

Support by the National Creative Research Initiatives of Ministry of Science and Technology, Korea.

Accepted for publication October 12, 2004.

Supplemental information can be found at <http://ajp.amjpathol.org>.

Address reprint requests to Sunghoon Kim, Center for ARS Network, College of Pharmacy, Seoul National University, San 56-1, Shillim-dong, Kwanak-gu, Seoul 151-742, Korea. E-mail: sungkim@snu.ac.kr.

avertin (100  $\mu$ l/10 g), shaved the dorsum, and disinfected the skin with 70% alcohol. A 0.5-cm-diameter circle was marked on the skin of the mid-dorsal region, and full-thickness excisional wounds, including the skin and panniculus carnosus muscle, were created using scissors.<sup>11</sup> The wounds were left uncovered without a dressing. One wound was generated per mouse. After wounding, we sacrificed the mice at various time intervals for histological analyses. We also treated the wounds with different forms of p43, at the indicated concentrations in phosphate-buffered saline (PBS) with 20% glycerol, twice a day at 12-hour intervals until day 3 after wounding. The wound closure was monitored daily, using the Image-pro Plus software, and was calculated as the percentage of the initial wound area. We isolated the wounds from the mice, and immediately fixed the tissue overnight in 10% formaldehyde. The fixed tissue was dehydrated and embedded in paraffin. We then sliced the embedded tissues with a microtome (Leica), and mounted them on silane-coated slides. The mounted tissues were dewaxed, rehydrated, stained with hematoxylin and eosin, and observed by microscopy (Nikon TE300). Separate sections were also stained with Masson's trichrome to evaluate the extent of collagen bundle formation in each wound.

### *Immunofluorescence Staining*

We fixed the isolated wounds with 4% paraformaldehyde at 4°C overnight. The tissues were washed with PBS, incubated in 30% sucrose for 4 hours, and finally frozen at -70°C in optimal cutting temperature (OCT) compound. The frozen sections (6  $\mu$ m) were attached to silane-coated slides, treated with PBS, blocked with PBS containing 0.1% Tween 20 and 1% skim milk, and reacted with antibodies specific to p43, MOMA-2 (Serotec), and Ki67 (Santa Cruz Biotechnology) at 37°C for 2 hours. We washed the slides with PBS containing 0.1% Tween 20 and incubated them at 37°C for 1 hour with the fluorescein isothiocyanate (FITC)-conjugated secondary antibody. The nuclei were counterstained with propidium iodide (10  $\mu$ g/ml) for 10 minutes, and the sections were examined under the confocal immunofluorescence microscope ( $\mu$ -Radiance; BioRad).

### *p43 Secretion Test*

We cultivated RAW264.7 and HaCAT cells ( $5 \times 10^4$  cells per 60-mm dish) for 16 hours and serum-starved them for 2 hours. TNF- $\alpha$  or interferon- $\gamma$  was added at 10 ng/ml, and cultured for 20 hours. We then harvested the culture media, which were clarified by centrifugation at  $4000 \times g$  for 15 minutes and concentrated by Viva spin ultrafiltration devices (molecular cutoff 10 kd; Vivascience). The proteins were separated by 10% sodium dodecyl sulfate (SDS)-polyacrylamide gel electrophoresis (PAGE) and the p43 in the media was detected by Western blotting with its specific antibody. Tubulin was used to monitor the cell lysis during the procedure. We also obtained the exudate from the wound area at various time intervals, and the presence of p43 was tested by Western blotting.

### *Preparation of p43*

We purified the His-tagged, 312-amino acid full-length p43 protein and the 146-amino acid N-terminal and 166-amino acid C-terminal domains of p43 as previously described, with a slight modification.<sup>12</sup> These proteins were expressed in *Escherichia coli* BL21 (DE3) by isopropylthio- $\beta$ -D-galactoside induction, and the cells were lysed by ultrasonication. After removing the cell debris by centrifugation at  $25,000 \times g$ , the supernatants were subjected to nickel affinity chromatography, and the proteins were purified following the protocol provided by the manufacturer (Invitrogen). Recombinant human platelet-derived growth factor (PDGF) was purchased from Sigma.

### *Cell Proliferation and Migration Assay*

We monitored the p43-dependent cell proliferation by measuring the incorporation of [<sup>3</sup>H] thymidine or BrdU to the replicating DNA as well as by directly counting cell numbers. We plated the indicated cells ( $5 \times 10^3$  cells) on 24-well dish, cultivated them for 12 hours, and serum-starved them for 3 hours. We then added the indicated amount of p43 to each well, and cultivated for 12 hours. After 4 hours of incubation with tritium-labeled thymidine (1  $\mu$ Ci/well), the cultured cells were washed with PBS three times, fixed with 5% TCA for 10 minutes, and washed again with PBS three times. We lysed the cells with 0.5 N NaOH and quantified the incorporated thymidine with a liquid scintillation counter (LKB). To measure the *in vivo* effect of p43 on the proliferation of dermal fibroblasts, we counted the total cells in the wounds per  $\times 60$  area by the PI signals and the proliferative cells by the Ki67-positive green cells. For the mean value, the Ki67-positive cells in at least four different areas were counted. We also determined the cell proliferation by measuring the BrdU incorporation. The same number of Detroit 551 cells was cultivated in Dulbecco's modified Eagle's medium with 10% fetal bovine serum overnight, serum-starved for 24 hours, and treated with the indicated concentrations of p43 for 48 hours. BrdU (10  $\mu$ mol/L) was incubated with the cells for 5 hours, and the cell proliferation was determined by the absorbance at 450 nm, using a Microplate reader (Bio-Rad model 550). The effect of p43 on cell proliferation was also determined by direct cell counting. Foreskin fibroblast cells ( $4 \times 10^4$ ) were cultured on a six-well dish for 12 hours and serum-starved for 24 hours. The cells were cultured in media containing 0.5% fetal bovine serum with vehicle or 100 nmol/L of p43 for the indicated times, trypsinized, and stained with trypan blue. We counted the cell numbers with a hemocytometer.

### *Binding of Biotin-Labeled p43 to Foreskin Fibroblasts*

Recombinant p43 (1.4 mg) was biotinylated with sulfo-NHS-biotin (Pierce), and was incubated on ice for 2 hours with 0.1 mg/ml of sulfo-NHS-SS-biotin (Pierce) in PBS. The remaining biotin was quenched with 100 mmol/L Tris

buffer (pH 7.5) and then the reaction solution was dialyzed in PBS. Foreskin fibroblasts ( $5 \times 10^3$  cells) were seeded onto a 12-well dish containing 9 × 9-mm coverslips, and cultured for 12 hours in Dulbecco's modified Eagle's medium with 10% fetal bovine serum and 1% streptomycin-penicillin. The medium was changed to serum-free medium containing 1% streptomycin-penicillin and 2% bovine serum albumin, and then the cultures were further incubated for 3 hours. The culture plates were incubated for 30 minutes at room temperature, and 50 nmol/L of biotin-labeled p43 (with 100  $\mu\text{g/ml}$  of anti-p43 polyclonal antibody or 1  $\mu\text{mol/L}$  native p43) was added to the culture medium and incubated for 20 minutes. The coverslips were washed three times with PBS to remove the unbound biotin-p43, and were blocked with 1% skim milk in PBS for 1 hour. The membrane bound biotin-p43 was captured with FITC-streptavidin, and the nuclei were stained with propidium iodide (500 ng/ml) for 1 hour at room temperature. The coverslips were washed three times with PBS and mounted with Gel/Mount (Biomed). The Biotinylated p43 bound to the foreskin fibroblasts was photographed ( $\times 60$ ) under confocal microscopy.

#### *Determination of Erk and JNK Activation*

Foreskin fibroblasts ( $6 \times 10^5$  cells) were plated in 100-mm dishes, cultivated for 12 hours, and serum-starved for 5 hours. Then, we added 100 nmol/L of p43, harvested the cells at the indicated times, lysed the cells in lysis buffer (50 mmol/L HEPES, pH 7.5, 150 mmol/L NaCl, 10% glycerol, 5 mmol/L EGTA, 1 mmol/L sodium orthovanadate, 10 mmol/L NaF, 12 mmol/L  $\beta$ -glycerophosphate, 1 mmol/L dithiothreitol, 1 mmol/L phenylmethyl sulfonyl fluoride, 5  $\mu\text{g/ml}$  aprotinin, and 1% Nonidet P-40), and centrifuged the lysates for 15 minutes at  $26,000 \times g$ . We separated the proteins in the cell lysates (20  $\mu\text{g}$ ) by 10% SDS-PAGE and performed immunoblotting with phospho-Erk and -JNK-specific antibodies. The fibroblasts ( $6 \times 10^5$  cells) were plated in 100-mm dishes, cultivated for 12 hours, serum-starved for 3 hours, and treated with 30  $\mu\text{mol/L}$  of U0126, 10  $\mu\text{mol/L}$  of PP2, 10  $\mu\text{mol/L}$  of SB202190, and 10  $\mu\text{mol/L}$  of LY294002 for 2 hours. Afterward, p43 was added to a 100 nmol/L concentration, and the cultures were further incubated for 30 minutes. We then measured the phosphorylation of Erk by immunoblotting with an anti-phospho-Erk antibody.

#### *Determination of Collagen Production*

Foreskin fibroblast cells ( $5 \times 10^4$  cells) were plated in a six-well dish, cultured for 12 hours, and serum-starved for 3 hours. We then added the indicated concentrations of p43 for 6 hours [reverse transcriptase-polymerase chain reaction (RT-PCR)] and 12 hours (Western blotting). We harvested the cells, lysed them with lysis buffer (50 mmol/L HEPES, pH 7.5, 150 mmol/L NaCl, 10% glycerol, 5 mmol/L EGTA, 1 mmol/L sodium orthovanadate, 10 mmol/L NaF, 12 mmol/L  $\beta$ -glycerophosphate, 1 mmol/L dithiothreitol, 1 mmol/L phenylmethyl sulfonyl fluoride, 5  $\mu\text{g/ml}$  aprotinin, and 1% Nonidet P-40), and centrifuged

the lysates for 15 minutes at  $26,000 \times g$ . We separated the cell lysates (30  $\mu\text{g}$ ) by 8% SDS-PAGE and performed immunoblotting with anti-collagen I and anti-tubulin antibodies. For RT-PCR of the collagen type I transcript, we isolated total RNA with TRIzol (Invitrogen) and performed RT-PCR using the specific primers.

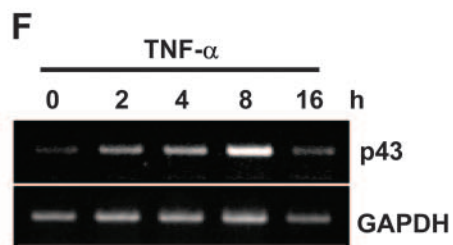
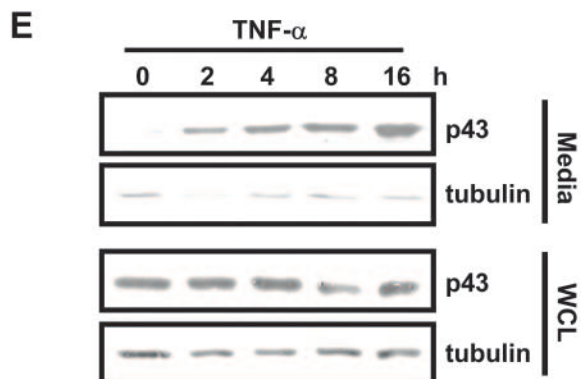
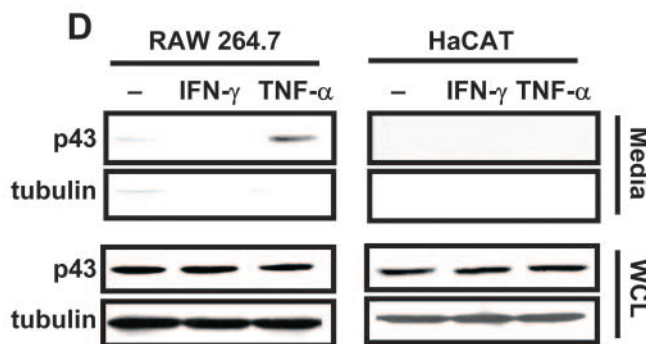
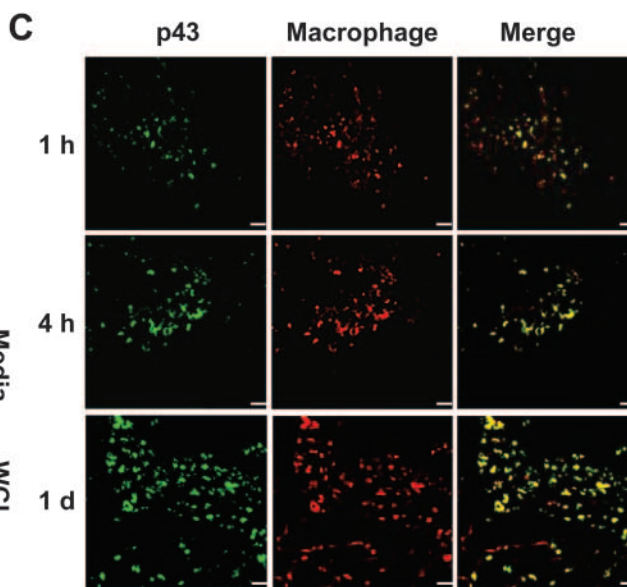
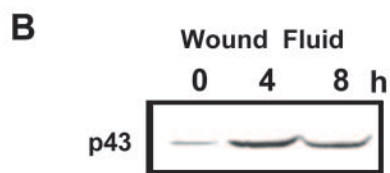
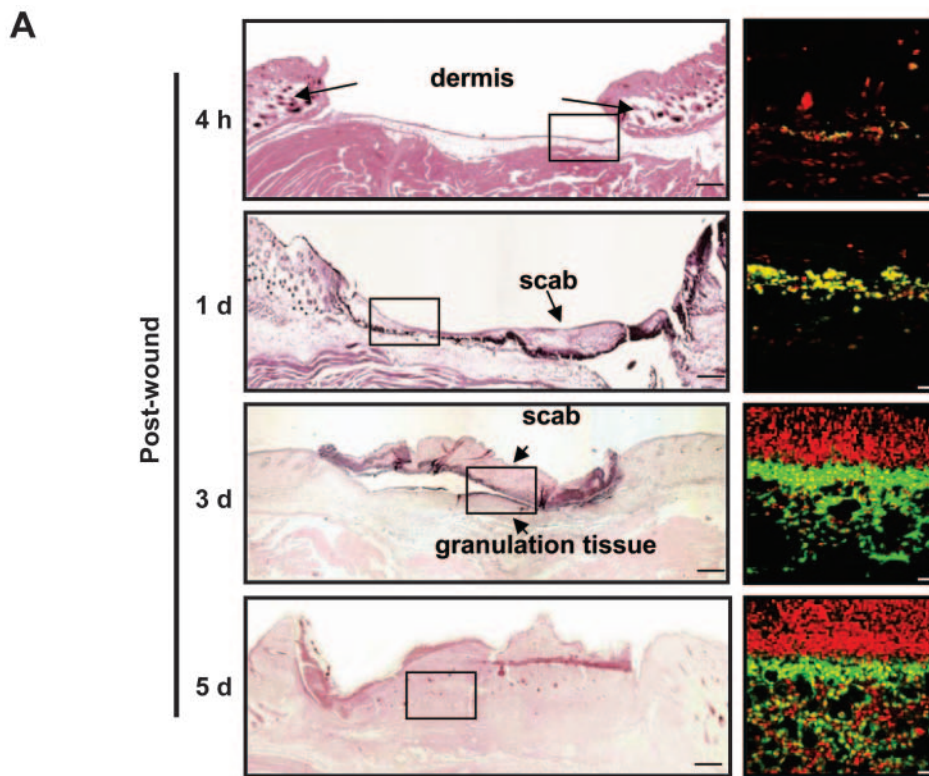
#### *Determination of TNF- $\alpha$ and p43 in Wound Exudates*

We introduced excisional wounds in the dorsal skin (diameter, 1 cm) of the p43<sup>+/+</sup> and p43<sup>-/-</sup> mice ( $n = 2$ ) as above, and immediately washed with PBS to remove the cell debris. We harvested the wound exudates by washing the wound areas with PBS at the indicated times, and centrifuging the solutions at  $4000 \times g$  for 15 minutes. We precipitated the wound exudates with 10% TCA, fractionated the proteins by 15% SDS-PAGE, and performed Western blotting with anti-TNF- $\alpha$  and anti-p43 antibodies.

### **Results**

#### *Enrichment of p43 at Wound Site*

To address the biological function of p43 during wound healing, we excised the full-thickness dorsal skin of mice and monitored whether the p43 level changed at the wound site. The level of p43 rapidly increased on wounding and reached a peak on day 3 (Figure 1A). The accumulation of p43 in the wound area was also confirmed by Western blotting of the wound fluid (Figure 1B). To identify the source of the p43, we compared the localization of p43 with those of the macrophages and endothelial cells recruited to the granulation tissue. This examination, revealed that p43 was co-localized with the MOMA2-positive cells<sup>13</sup> that are known to be macrophages (Figure 1C), but not with the endothelial cells (Supplementary Figure 1 at <http://ajp.amjpathol.org>). To determine whether the recruited macrophages are responsible for the secretion of p43, we checked the secretion of p43 from macrophages in response to TNF- $\alpha$ , which is elevated on wounding.<sup>14,15</sup> TNF- $\alpha$  enhanced the secretion of p43 from macrophage RAW264.7 cells, but the secretion of p43 was not observed from the untreated or interferon- $\gamma$ -treated RAW264.7 cells or from HaCAT keratinocytes (Figure 1D). We then monitored the time course of the TNF-induced secretion of p43 in RAW264.7 cells, and also checked whether the expression of p43 is induced by TNF- $\alpha$ . The secreted p43 was observed in media from 2 hours after the TNF- $\alpha$  treatment, and accumulated in a time-dependent manner (Figure 1E, top), whereas the intracellular level of p43 hardly changed (Figure 1E, bottom). To see whether the expression of p43 is induced by TNF- $\alpha$ , we measured the amount of the p43 transcript by RT-PCR. The transcript level was increased after the p43 treatment up to 8 hours and then decreased (Figure 1F). Thus, the



induction of p43 appears to be necessary to compensate for the loss of intracellular p43 because of its secretion.

### Stimulation of Fibroblast Proliferation by p43

To understand the function of p43, we checked the effect of p43 on the proliferation of various cell types that would be present in the wound area. p43 increased the proliferation of foreskin fibroblasts in a dose-dependent manner (Figure 2A), whereas it suppressed bovine aorta endothelial cell proliferation (Figure 2B), as we previously reported.<sup>9</sup> Interestingly, the proliferative activity was localized to the 146-amino acid N-terminal region of p43 (Figure 2A), whereas both of the N- and C-terminal domains showed the suppressive activity on the endothelial cell proliferation (Figure 2B). However, p43 did not have any effect on the proliferation of human keratinocytes, HaCAT (Figure 2C), osteoblasts, U2OS (Figure 2D), and different immune cells (Supplementary Figure 2 at <http://ajp.amjpathol.org>), indicating that the proliferative activity of p43 is specific to fibroblasts. To determine the apparent ED<sub>50</sub> of p43 in cell proliferation, we treated Detroit 551 cells with different concentrations of p43, and generated a dose-response curve. The proliferative activity of p43 increased in a dose-dependent manner and showed the peak activity at 200 nmol/L (Figure 2E). Based on this graph, the apparent ED<sub>50</sub> appears to be ~85 nmol/L. We then compared the proliferative activity of p43 with the known growth factor, PDGF. p43 showed a dose-dependent increase in its proliferative activity, whereas PDGF demonstrated the peak activity at the 1 nmol/L concentration (Figure 2F). A similar result was also obtained when the cell proliferation was monitored by cell division (Figure 2G). We then determined whether p43 induces the migration of fibroblasts using a Trans-well chamber. Although the cell migration was enhanced by PDGF, p43 did not increase fibroblast migration (Figure 2H). Together, these results demonstrate that p43 specifically stimulates the proliferation of dermal fibroblasts, but does not appear to trigger the migration of these cells.

### Erk Mediates p43-Dependent Proliferation of Fibroblasts

We then checked the binding of p43 on foreskin fibroblasts. The binding of biotin-labeled p43 was observed by immunofluorescence staining with FITC-conjugated secondary antibody (Figure 3Aa). The cell binding of p43 was blocked by a titration with an anti-p43 antibody or unlabeled p43 (Figure 3A, b and c), and the FITC-conju-

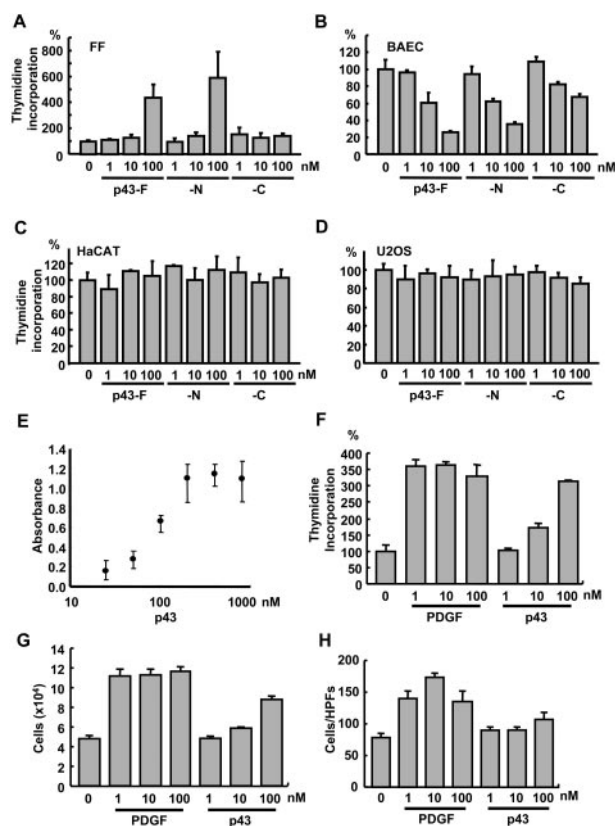


**Figure 2.** p43 promotes fibroblast proliferation and collagen production. The effect of the 312-amino acid full-length (F), and 146-amino acid N-terminal domain and 166-amino acid C-terminal domain of p43 on the proliferation of foreskin fibroblasts (A, FF), bovine aorta endothelial cells (B, bovine aorta endothelial cells), keratinocytes (C, HaCAT), and osteoblasts (D, U2OS). The proliferation was monitored by the incorporation of [<sup>3</sup>H] thymidine into the cells, and the proliferation of the untreated cells was taken as 100%. The values stand for the average of three independent experiments. **E:** The fibroblast Detroit 551 cells were treated with the indicated concentrations of p43 (twofold increases from 25 nmol/L) to obtain the dose-response curve. The cell proliferation was determined by measuring the incorporated BrdU at 450 nm, as described in the Materials and Methods. The experiments were repeated three times. **F:** Foreskin fibroblasts were treated with the indicated concentrations of PDGF and p43. The cell proliferation was monitored by thymidine incorporation (*n* = 3). **G:** The effects of PDGF and p43 on the cell proliferation of foreskin fibroblasts were also monitored by counting the cell numbers after treatments with different concentrations of these factors (*n* = 3). **H:** The PDGF and p43 activities on the migration of foreskin fibroblasts were determined using a Trans-well chamber (8 μm, Costar) coated with type I collagen as described in the Materials and Methods. The migrated cells were visualized by staining with hematoxylin and were counted in high-power fields (×20). The experiments were repeated three times.

gated secondary antibody alone did not show cell binding (Figure 3Ad), indicating that the fluorescent signal is because of the specific cell binding of p43. We also determined the time course of p43 binding to foreskin fibroblasts. The exogenously added p43 bound to the

**Figure 1.** Secretion of p43 from macrophages at the wound site. **A:** A 0.5 cm diameter, full-thickness portion of the dorsal skin was removed, and cross sections of the wound area were stained with H&E at the indicated times after wounding. The boxed regions were stained with anti-p43 antibody (green) and propidium iodide (red), and were observed by immunofluorescence microscopy. **B:** The accumulation of p43 in wound fluid was detected by Western blotting with an anti-p43 antibody. We obtained the wound fluids by washing the skin wound regions with PBS at the indicated times, precipitating the proteins with 10% TCA, and separating them by SDS-PAGE for Western blotting. **C:** The isolated granulation regions were reacted with anti-p43 and anti-MOMA2 antibodies<sup>13</sup> at the indicated times after wounding to visualize p43 and macrophages, respectively. The p43 and macrophages were then stained with FITC- and TRITC-conjugated secondary antibodies, respectively. **D:** The macrophages (RAW264.7) and keratinocytes (HaCAT) were cultivated and treated with 10 ng/ml of TNF-α or interferon-γ, and the expression and secretion of p43 were determined by Western blotting of the whole cell lysates (WCL) and culture media, respectively. **E:** Time course of the TNF-dependent secretion (top) and the intracellular level (bottom) of p43 in RAW264.7 cells. The secretion of p43 into the culture medium was monitored as above. A trace amount of tubulin was present in medium because of cell lysis during the experiment. **F:** The time-dependent induction of p43 was determined by RT-PCR of the p43 transcript after the TNF-α treatment. Scale bars: 250 μm (A); 25 μm (boxed regions in A, C).

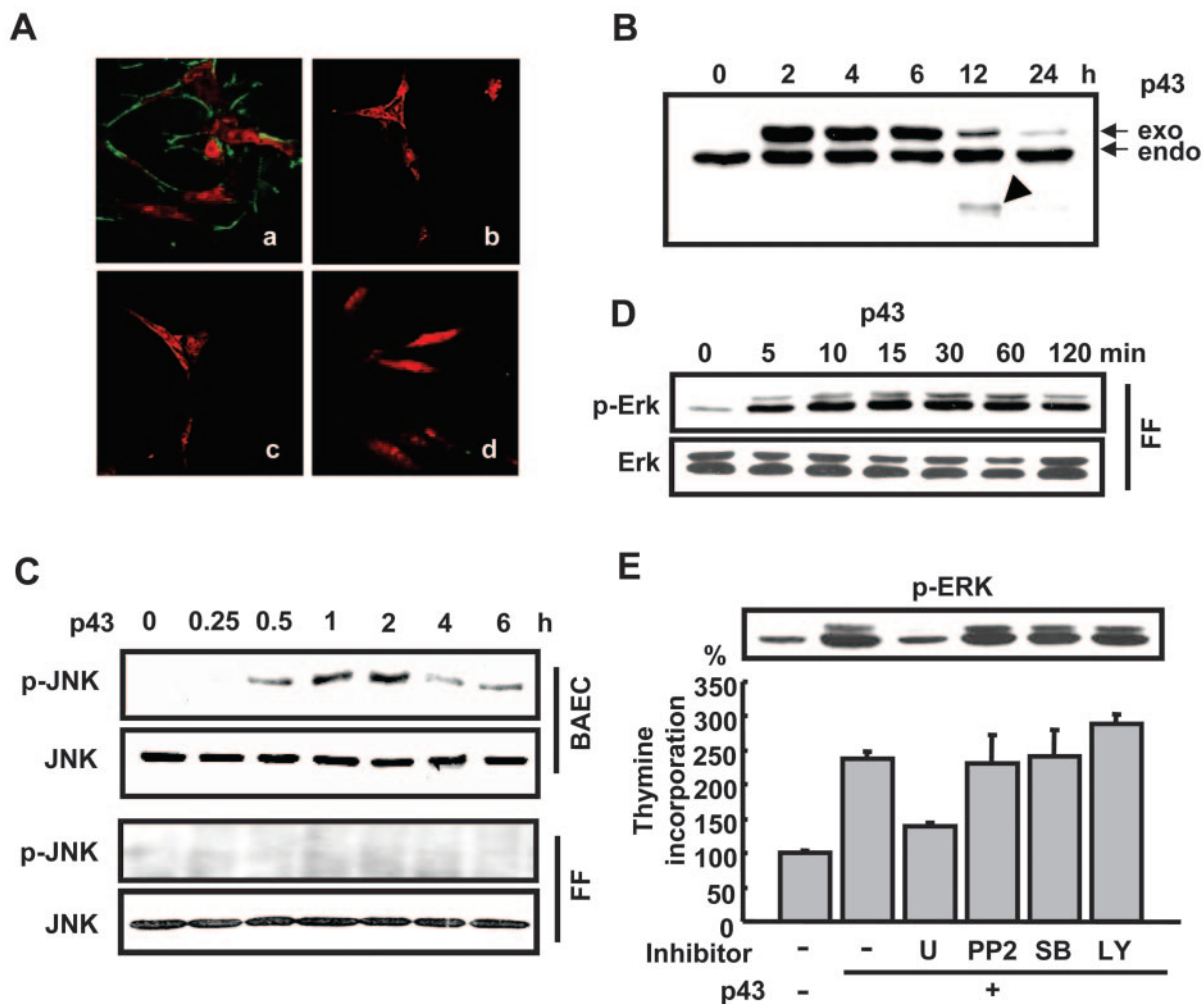


**Figure 3.** Erk is responsible for the p43-induced proliferation of fibroblasts. **A:** Foreskin fibroblasts were cultivated in the presence of biotin-labeled p43. The cell binding specificity of biotin-p43 was determined by titrations with anti-p43 antibody or native p43. **a:** Biotin-p43 alone treated; **b:** biotin-p43 and anti-p43 antibody treated; **c:** biotin-p43 and native p43 treated; **d:** FITC-conjugated secondary antibody alone treated. **B:** The time course of p43 binding to foreskin fibroblasts was determined by Western blotting of the cell extracts. Foreskin fibroblasts were cultivated in the presence of 100 nmol/L p43, and were harvested at the indicated times. The total protein extracts were prepared from the harvested cells, and the levels of exogenously treated His-tagged (exo) and endogenous (endo) p43 were determined by Western blotting with the anti-p43 antibody. Note that the degradation band of p43 (arrowhead) is detected in the cells harvested at 12 hours after p43 treatment. **C:** Time course of p43-dependent JNK activation in bovine aorta endothelial cells and foreskin fibroblasts. The cultivated cells were treated with 100 nmol/L of p43 and were harvested at the indicated times. The levels of phosphorylated and total JNK were determined by Western blotting with their respective antibodies. **D:** The p43-dependent activation of Erk was monitored in foreskin fibroblasts. The cells were treated with 100 nmol/L of p43, and were harvested as above, and the amounts of phosphorylated and total Erk were determined by immunoblotting with their specific antibodies. **E:** The effects of various kinase inhibitors on the phosphorylation of Erk induced by p43. Foreskin fibroblasts were pretreated with U0126 (30  $\mu$ mol/L), PP2, SB202190, and LY294002 (each at 10  $\mu$ mol/L), and were subsequently treated with 100 nmol/L of p43. Then, the phosphorylation of Erk was determined by immunoblotting, as described above. U0126, PP2, SB202190, and LY294002 are the inhibitors of ERK kinase, Src, two other MAPKs (p38 MAPK and JNK), and PI3K, respectively.

cells within 2 hours, and its level was decreased after 6 hours, whereas the level of endogenous p43 remained unchanged (Figure 3B).

In our previous work, we found that p43 activates Jun N-terminal kinase (JNK) and extracellular signal-regulated kinase (Erk) in immune and endothelial cells.<sup>9,16</sup> Here, we checked whether p43 also activates these kinases in foreskin fibroblasts as well as in bovine aorta endothelial cells. Although it induced the phosphorylation of JNK in bovine aorta endothelial cells, it had little effect on JNK in fibroblasts (Figure 3C, top), indicating that JNK is not responsible for the p43-induced proliferation of fibroblasts. In contrast, the phosphorylation of Erk was enhanced by p43, and reached its peak level within 30 minutes after the p43 treatment (Figure 3D). Suppression

of Erk with its inhibitor, U0126, specifically blocked the p43-induced cell proliferation, whereas other kinase inhibitors had little effect (Figure 3E), suggesting that Erk mediates the proliferative signal of p43 in fibroblasts.

### Exogenous p43 Promotes Wound Repair

We then tested whether the proliferative activity of p43 on fibroblasts could be reproduced *in vivo*. After introducing a full-thickness excisional wound on the dorsal skin of mice, we treated the wounds with p43 twice a day for 3 days. We then monitored whether supplementation with p43 would promote the overall wound healing process. On day 3 after wounding, the wound areas treated with

p43-F or p43-N were reduced to ~40% of the initial size of the wound, whereas those treated with vehicle or p43-C were still ~70% of the size of the initial wounds (Figure 4A). We sacrificed the mice 3 days after wounding, and checked the proliferation of dermal fibroblasts by immunofluorescence staining with the anti-Ki67 antibody, which recognizes a marker of proliferation.<sup>17</sup> The full-length and N-terminal domain of the p43 protein increased the number of proliferating dermal skin fibroblasts, whereas its C-terminal domain did not (Figure 4B), consistent with the activity of p43 on fibroblasts determined *in vitro* (Figure 2A). Because fibroblasts are an important source of collagen during wound repair, we also examined whether collagen production is induced in fibroblasts by p43, using RT-PCR and Western blot analyses. The collagen production from fibroblasts was significantly elevated by p43 treatment, in dose- and time-dependent manners (Figure 4, C and D).

### Generation and Characterization of p43<sup>-/-</sup> Mice

To confirm that p43 is functionally nonredundant and a critical factor for wound healing, we generated p43-deficient mice through the gene trap method, as previously described.<sup>18,19</sup> Using Southern blotting and genomic PCR, we confirmed the insertion of the gene trap vector into the p43 gene (Supplementary Figure 3A at <http://ajp.amjpathol.org>). The insertion of the gene trap vector sufficiently inhibited the expression of p43, as determined by Northern and Western blot analyses (Supplementary Figure 3B at <http://ajp.amjpathol.org>). The exact location of the gene trap insertion was confirmed by sequencing (Supplementary Figure 3C at <http://ajp.amjpathol.org>). The intercross of the heterozygotes generated wild-type, heterozygous, and homozygous offspring at a ratio of 1:3.3:1.8 ( $n = 97$ ), and the newborn homozygous pups showed normal gross morphology, suggesting that the mutation does not cause serious defects or lethality during embryogenesis. Because p43 was first identified as a component of the multi-tRNA synthetase complex that contains several different tRNA synthetases essential for the translation process, we checked whether overall protein synthesis was damaged by the depletion of p43. The cellular protein synthesis was monitored by the incorporation of radioactive methionine into nascent polypeptides, as determined by autoradiography and scintillation counting of the total proteins. In both assays, few differences were observed between the wild-type and mutant cells (Supplementary Figure 3, D and E, at <http://ajp.amjpathol.org>). Because protein synthesis *in vivo* is mainly controlled by the phosphorylation of eIF2 $\alpha$ , which is the key regulator for translational initiation,<sup>20</sup> the phosphorylation of eIF2 $\alpha$  was also compared by Western blotting with an anti-phospho-eIF2 $\alpha$  antibody. The result did not reveal apparent differences in the phosphorylation of eIF2 $\alpha$  (Supplementary Figure 3F at <http://ajp.amjpathol.org>). All of these results suggest that the rate of protein synthesis may not be significantly

affected by a deficiency in p43, at least in cells cultivated in complete media.

To determine whether the cell growth is affected by the lack of p43, the growth rates of the p43<sup>+/+</sup> and p43<sup>-/-</sup> cells were compared using isolated mouse embryonic fibroblasts (MEFs). The same number of cells was seeded, and the cell numbers were counted after 2 days of cultivation. Then, the same cell numbers were diluted into fresh media, and the same cultivation was repeated for seven passages. The accumulated population doubling of p43<sup>+/+</sup> and p43<sup>-/-</sup> cells was calculated as described previously,<sup>21,22</sup> and is displayed as a line graph. This comparison showed that the wild-type and p43<sup>-/-</sup> MEF cells grow at a similar rate (Supplementary Figure 3G at <http://ajp.amjpathol.org>). Based on these results, we concluded that the depletion of p43 would have minimal effects on the isolated fibroblasts, in terms of protein synthesis and proliferation.

### Retardation of Wound Repair by Depletion of p43

To determine the functional significance of p43 in wound repair, we generated the dorsal skin wound as above and compared the wound closure in the p43<sup>+/+</sup> and p43<sup>-/-</sup> mice. The wound healing rate was significantly delayed in the p43<sup>-/-</sup> mice (Figure 5, A and B). This result proves the functional significance of p43 in the wound repair process and implies that the p43 function is not compensated by other growth factors or cytokines *in vivo*. To see whether the retarded wound repair in the p43<sup>-/-</sup> mice could be assisted by exogenous supplementation with p43, we generated the skin injury in p43<sup>+/+</sup> and p43<sup>-/-</sup> mice as above, and compared the effect of p43 on the healing process. The treatment with exogenous p43 significantly enhanced the wound closure in both the p43<sup>+/+</sup> and p43<sup>-/-</sup> mice (Figure 5C), proving that the depletion of the endogenous p43 was compensated by the exogenous supplementation with p43 in wound repair, although the wound closure of the p43<sup>-/-</sup> mice was still retarded as compared to that of the wild-type mice, even after the exogenous p43 treatment. The immunofluorescence staining of the wound region showed that the number of proliferating fibroblasts decreased with the depletion of endogenous p43, and recovered by the supplementation with p43 (Figure 5D, top). The number of Ki76-positive proliferating cells was increased by approximately twofold to fourfold by the treatment with p43 in both p43<sup>+/+</sup> and p43<sup>-/-</sup> mice (Figure 5D, bottom). Because p43 also induced collagen production in cultivated fibroblasts (Figure 4, C and D), we checked whether the collagen content in the wound region is affected by the p43 depletion or supplementation. As expected, the collagen level was severely reduced by the deficiency of endogenous p43 in p43<sup>-/-</sup> mice, but the application of p43 to the wound area enhanced the collagen production (Figure 5E), consistent with the *in vitro* results above. The recovery of the delayed wound healing by the exogenous supplementation of p43 in p43<sup>-/-</sup> mice suggests that the

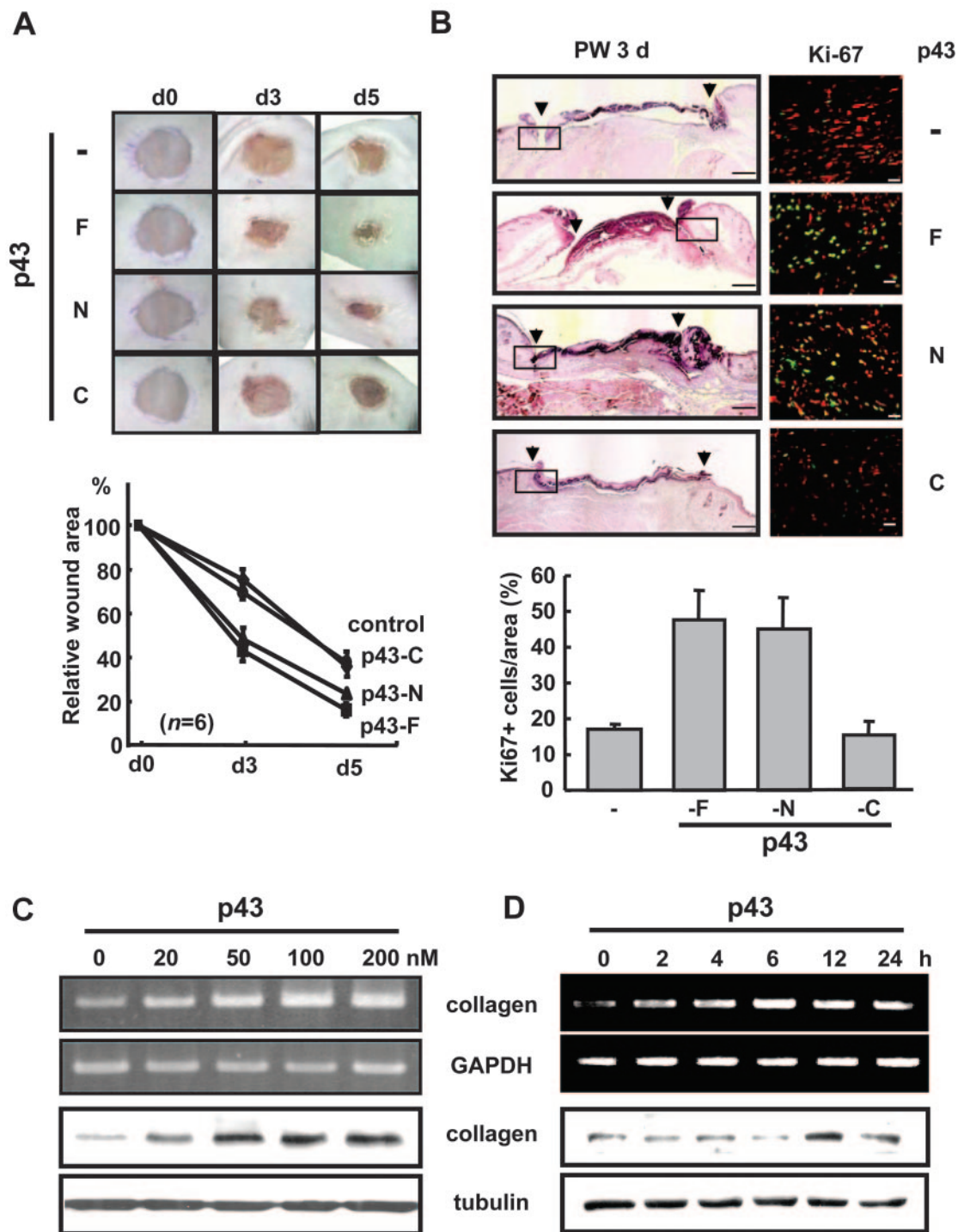


**Figure 4.** p43 stimulates fibroblast proliferation and collagen production for wound repair. **A:** The effects of the different forms of p43 on wound closure were evaluated at various time intervals (**top**), and the relative size of the determined wound area is shown as a line graph, taking the initial wound size as 100% (**bottom**). The wounds were generated on the dorsal skin of mice, as described above, and were treated with the same molar concentration of p43-F (4  $\mu\text{g}/\text{wound}$ ), p43-N (2.1  $\mu\text{g}/\text{wound}$ ), and p43-C (2.6  $\mu\text{g}/\text{wound}$ ) twice a day at after wounding at days 0, 2, and 4. The wound closure was monitored (**top**), and the relative sizes of the wounds are represented as a line graph (**bottom**). **B:** The wounds were treated with different forms of p43 twice a day for 3 days (PW 0, 1, and 2). The 3 day after wound tissues were isolated, and cross sections of the wound area were subjected to H&E staining. The re-epithelialization regions in the wounds (marked with **boxes**) were stained with the anti-Ki67 antibody and PI to visualize the proliferating fibroblasts (green) and the nuclei (red), respectively. The Ki-67-positive (green) and total (red) cells were counted in four different wound areas of 0.044  $\text{mm}^2$ , and the percentages of the proliferating cells were averaged and are demonstrated by bar graphs. **C:** The time course of p43-induced collagen production in foreskin fibroblasts was monitored by RT-PCR of collagen type I transcript (**top**), and Western blotting with an anti-collagen type I antibody (**bottom**). **D:** The dose-dependent induction of collagen by p43 was also determined, as described above. Scale bars: 1 mm (**A**); 25  $\mu\text{m}$  (**boxed regions** in **A**).

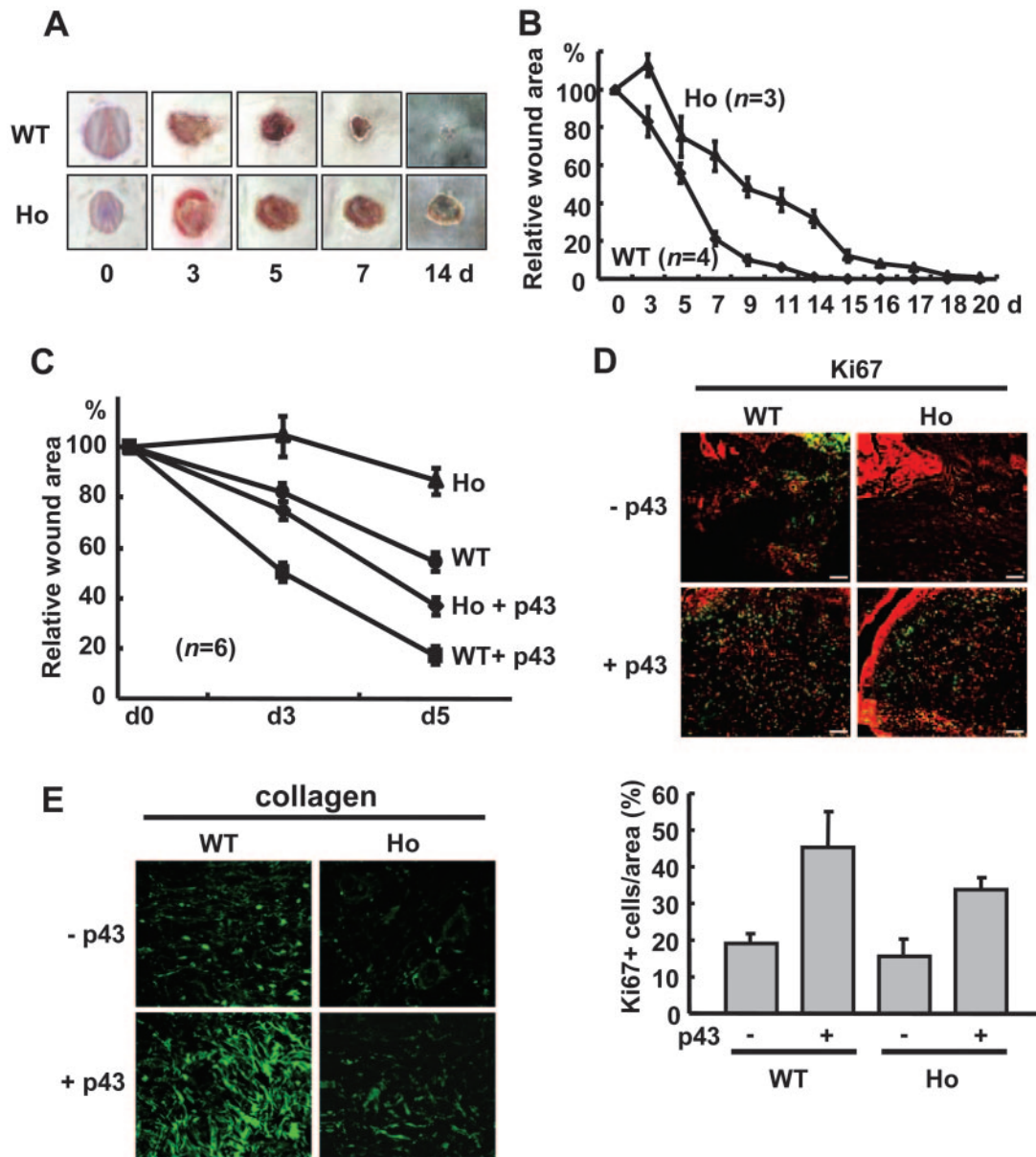


**Figure 5.** Depletion of endogenous p43 retards wound healing. **A:** The wound closure by the  $p43^{+/+}$  and  $p43^{-/-}$  mice was compared at various time intervals. **B:** The change in the average wound area is represented by a line graph. **C:** The effect of p43 on the wound closure in the  $p43^{+/+}$  and  $p43^{-/-}$  mice. The excisional wounds were generated on the dorsal skin of the  $p43^{+/+}$  and  $p43^{-/-}$  mice, treated with p43 at the concentration of  $4 \mu\text{g}/\text{wound}$ , and the wound closure was monitored as above. **D, top:** The re-epithelialization regions in the wounds were subjected to immunofluorescence staining with the anti-Ki67 antibody and PI to determine the proliferation of dermal fibroblasts (green) and nuclei (red), respectively. **D, bottom:** The Ki-67-positive (green) and total (red) cells were counted in the three different wound areas of  $0.39 \text{ mm}^2$ , and the percentages of the proliferating cells were averaged and are demonstrated by bar graphs. **E:** The amount of collagen in the re-epithelialization regions was compared by immunofluorescence staining with an anti-collagen antibody. Scale bars,  $100 \mu\text{m}$  (**D**).

functional activity of p43 in wound healing is exerted by its extracellular cytokine activity.

### Histological Analysis of the Effect of p43 on Wound Healing

To further confirm the significance of p43 in wound healing, we also compared the effects of p43 deficiency and exogenous supplementation on wound healing by histological analysis. After the creation of the full-thickness excisional wounds, the rate of wound healing was markedly delayed in the p43-deficient mice, as shown above

(Figure 5A), with an impaired inflammatory response within 24 hours (data not shown) and a minimal fibroblastic response by day 3 (Figure 6A). The wounds of the  $p43^{-/-}$  mice displayed fewer fibroblasts and less granulation tissue, as compared with the wild-type controls (Figure 6A). In both cases, the exogenous supplementation with p43 increased the density of fibroblasts. A significant difference in the re-epithelialization level, however, was not observed between  $p43^{-/-}$  and wild-type mice (data not shown). Thus, the retarded reduction of the wound area in the p43-deficient mice (Figure 5A) appears to result from minimal wound contraction be-

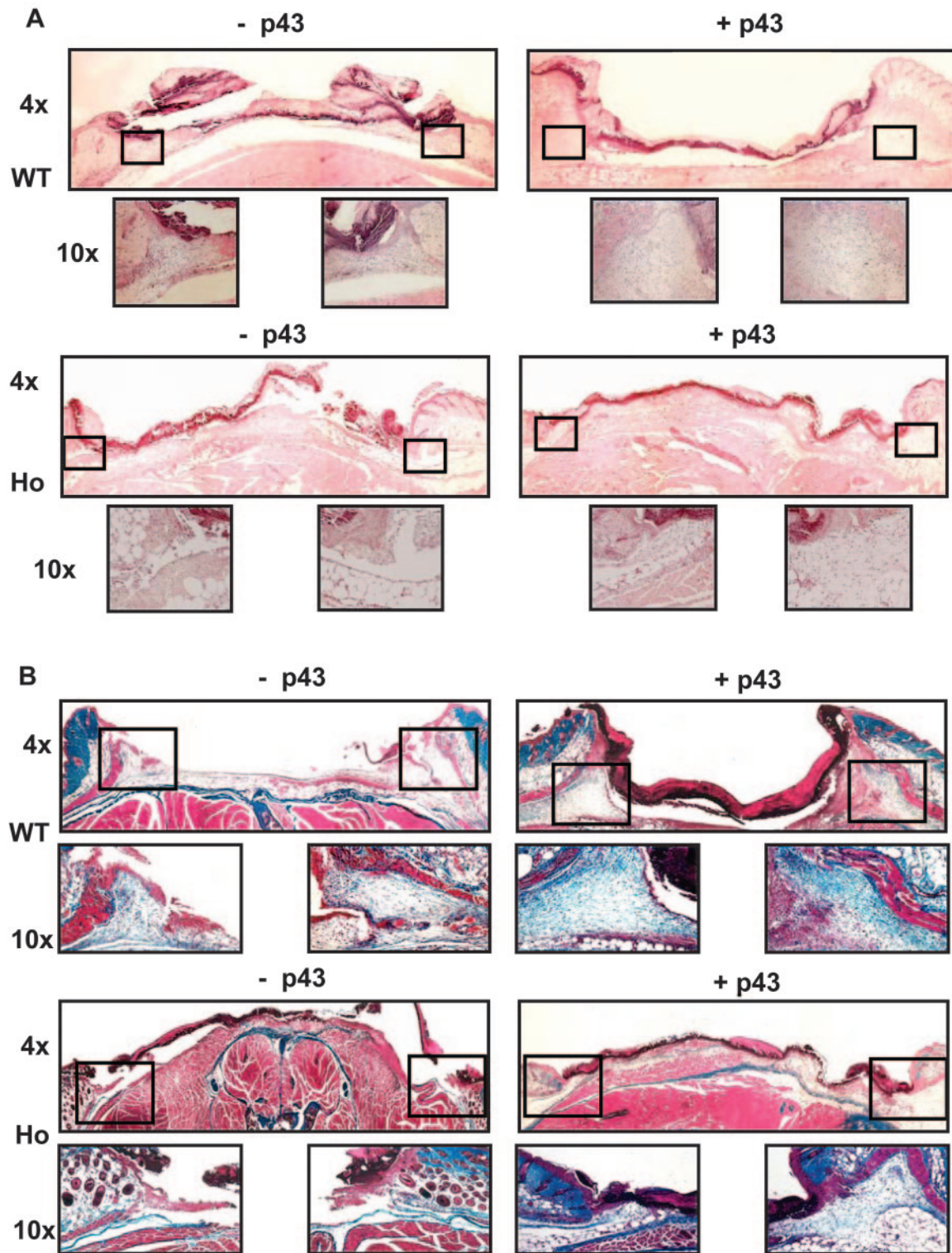


**Figure 6.** Histological analysis of p43 effect on wound healing. **A:** A 0.5 cm diameter full-thickness portion of the dorsal skin was removed and cross sections of the wound area were stained with H&E at day 3 after wounding. p43<sup>+/+</sup> and p43<sup>-/-</sup> mice were treated twice a day with vehicle or p43 (4  $\mu$ g/wound). Fibroblasts are rarely present in the wounds of p43-deficient mice, but are enriched by p43 treatment. **B:** The wound healing process was also monitored by Masson-trichrome staining. The deposition of ECM in the wound was severely decreased by the depletion of p43, and was increased by the exogenous treatment with p43. Original magnifications:  $\times 4$ ;  $\times 10$  (boxed regions).

cause of the lower number of fibroblasts, because wound contraction occurs through the contributions of re-epithelialization and contractability of wound fibroblasts. This interpretation is further strengthened by the Masson trichrome-staining results of the wound sections. This staining highlighted the decreased deposition of extracellular matrix in the wounds of p43<sup>-/-</sup> mice as compared to those of the wild-type mice, and its enhanced accumulation by the exogenous application of p43 (Figure 6B). Combined together, these histological analyses demonstrated results that are consistent with the stimulatory effect of p43 on fibroblastic activities and matrix deposition during wound healing.

## Discussion

The level of p43 rapidly increased up to 3 days after injury, and subsequently decreased (Figure 1; A to C), implying that it plays a significant role in the inflammation and proliferation stage during wound repair. We have previously shown that p43 itself can induce the expression of TNF- $\alpha$  in macrophages.<sup>6,7</sup> This work demonstrated that p43 is in turn induced and secreted from macrophages by TNF- $\alpha$  (Figure 1; D to F). Thus, p43 and TNF- $\alpha$  appear to form a positive feedback loop with each other to amplify the inflammatory response on tissue injury. When we monitored the accumulation of TNF- $\alpha$  in the wound exudates, the levels of TNF- $\alpha$  and p43 were both significantly increased in the wound exudates of the wild-type mice, in contrast to the p43-deficient wounds (Supplementary Figure 4A at <http://ajp.amjpathol.org>), further supporting the stimulatory relationship between the two proinflammatory factors in an autocrine manner. In contrast, the p43 secreted from the macrophages works on the proliferation of dermal fibroblasts in a paracrine mode.

The binding of p43 to fibroblasts is completed within 2 hours after the p43 treatment (Figure 3B). The gradual decrease of exogenous p43 may result from the dissociation of p43 from the cell or degradation after internalization. Among these possibilities, the latter seems to be the case, because we previously observed the internalization of p43 in various target cells (data not shown) and the degradation band of p43 appeared at 12 hours after p43 treatment (Figure 3B, arrowhead). We previously observed that p43 stimulates the migration, but not the proliferation, of endothelial cells.<sup>9</sup> However, we found in this work that p43 had minimal effects on the migration of fibroblasts, while it stimulated their proliferation (Figure 2). In addition, the proliferative activity on fibroblasts is expressed only in the N-terminal domain of p43, whereas its activities on immune and endothelial cells require the intact p43 protein structure<sup>6,9</sup> (Figure 2, A and B). Further deletion mapping revealed that its activity on endothelial cells appears to reside in the central region of p43, explaining why both the N- and C-terminal domains retained the activity (data not shown). p43 activates JNK in endothelial cells, but not in fibroblasts (Figure 3C). All of these results imply that p43 would work in fibroblasts via a receptor and mechanism distinct from those in other cells.<sup>7</sup> It is also unknown whether posttranslational mod-

ifications are involved in the different cytokine activities or potency of p43, because we used recombinant p43 produced in *E. coli*. We are currently investigating the structural relationship of p43 to its diverse biological activities.

It is plausible that a deficiency in p43 may reduce cellular protein synthesis or proliferation, because p43 facilitates the catalytic reaction of the bound tRNA synthetase.<sup>12</sup> However, the protein synthesis and proliferation of the isolated fibroblasts were barely affected by the deficiency of p43, at least in the complete media (Supplementary Figure 3, D to G, at <http://ajp.amjpathol.org>). Recently, we determined the functional significance of another tRNA synthetase-associating factor, p38, in protein synthesis and cell proliferation. Although this factor was essential for the assembly and stability of the component enzymes within the multi-tRNA synthetase complex, its absence did not affect the protein synthesis and proliferation of the isolated fibroblasts.<sup>23</sup> Thus, it is not so surprising that the depletion of p43 does not severely slow retard protein synthesis and cell proliferation. However, we cannot exclude the possibility that p43 may become more significant for protein synthesis under starving or stressful conditions. In addition, the retarded wound healing caused by the lack of endogenous p43 was at least partially compensated by the exogenous treatment with p43 in the p43<sup>-/-</sup> mice (Figure 5C), suggesting that the slower wound healing does not result from reduced cellular protein synthesis, and that the extracellular cytokine activity of p43 is mainly responsible for the wound-healing process.

Diverse growth factors, with distinct activity mechanisms, are involved in the process of wound healing at different stages. Among them, epidermal growth factor, fibroblast growth factor, PDGF, and transforming growth factor- $\beta$  have been relatively well studied.<sup>2</sup> In addition, proinflammatory cytokines can also promote wound repair by various processes. For instance, mice deficient in interleukin-6 displayed compromised cutaneous wound healing.<sup>24,25</sup> In this case, interleukin-6 indirectly stimulates keratinocyte migration via its activation of STAT3 in fibroblasts, which can induce some soluble factors. In contrast to interleukin-6, p43 directly stimulates fibroblast proliferation and collagen production. In addition, it also confers chemotactic activities to endothelial and immune cells.<sup>6,9</sup> In fact, the exogenous supplementation of p43 enhanced the accumulation of macrophages and endothelial cells in the wound area (Supplementary Figure 4B at <http://ajp.amjpathol.org>). Thus, all of these complex activities of p43 on fibroblasts as well as endothelial and immune cells can cooperatively facilitate the wound healing process. We anticipate that p43 will be a novel wound healing agent, which may work in combination with other previously characterized wound healing growth factors and cytokines.

## References

1. Singer AJ, Clark RAF: Cutaneous wound healing. *N Engl J Med* 1999, 341:738-746

2. Werner S, Grose R: Regulation of wound healing by growth factors and cytokines. *Physiol Rev* 2003, 83:835–870
3. Quevillon S, Agou F, Robinson J-C, Mirande M: The P43 component of the mammalian multi-synthetase complex is likely to be the precursor of the endothelial monocyte-activating polypeptide II cytokine. *J Biol Chem* 1997, 272:32573–32579
4. Han JM, Kim JY, Kim S: Molecular network and functional implications of macromolecular tRNA synthetase complex. *Biochem Biophys Res Commun* 2003, 303:985–993
5. Barnett G, Jakobsen AM, Tas M, Rice K, Carmichael J, Murray JC: Prostate adenocarcinoma cells release the novel proinflammatory polypeptide EMAP-II in response to stress. *Cancer Res* 2000, 60:2850–2857
6. Ko Y-G, Park H, Kim T, Lee J-W, Park SG, Seol W, Kim JE, Lee W-H, Kim S-H, Park JE, Kim S: A cofactor of tRNA synthetase, p43, is secreted to up-regulate proinflammatory genes. *J Biol Chem* 2001, 276:23028–23033
7. Chang SY, Park SG, Kim S, Kang CY: Interaction of the C-terminal domain of p43 and the alpha subunit of ATP synthase: its functional implication in endothelial cell proliferation. *J Biol Chem* 2002, 277:8388–8394
8. Park H, Park SG, Kim J, Ko YG, Kim S: Signaling pathways for TNF production induced by human aminoacyl-tRNA synthetase-associated factor, p43. *Cytokine* 2002, 20:148–153
9. Park SG, Kang YS, Ahn YH, Lee SH, Kim KR, Kim KW, Koh GY, Ko YG, Kim S: Dose-dependent biphasic activity of tRNA synthetase-associated factor, p43, in angiogenesis. *J Biol Chem* 2002, 277:45243–45248
10. Martin P: Wound healing—aiming for perfect skin regeneration. *Science* 1997, 276:75–81
11. Werner S, Smola H, Liao X, Longaker MT, Krieg T, Hofschneider PH, Williams LT: The function of KGF in morphogenesis of epithelium and reepithelialization of wounds. *Science* 1994, 266:819–822
12. Park SG, Jung KH, Lee JS, Jo YJ, Motegi H, Kim S, Shiba K: Precursor of pro-apoptotic cytokine modulates aminoacylation activity of tRNA synthetase. *J Biol Chem* 1999, 274:16673–16676
13. Kraal G, Rep M, Janse M: Macrophages in T and B cell compartments and other tissue macrophages recognized by monoclonal antibody MOMA-2. An immunohistochemical study. *Scand J Immunol* 1987, 26:653–661
14. Han YP, Tuan TL, Wu H, Hughes M, Garner WL: TNF-alpha stimulates activation of pro-MMP2 in human skin through NF-(kappa)B mediated induction of MT1-MMP. *J Cell Sci* 2001, 114:131–139
15. Winston BW, Krein PM, Mowat C, Huang Y: Cytokine-induced macrophage differentiation: a tale of 2 genes. *Clin Invest Med* 1999, 22:236–255
16. Park H, Park SG, Lee J-W, Kim T, Kim G, Ko Y-G, Kim S: Monocyte cell adhesion induced by a human aminoacyl-tRNA synthetase associated factor, p43: identification of the related adhesion molecules and signal pathways. *J Leukoc Biol* 2002, 71:223–230
17. Ben-Izhak O, Bar-Chana M, Sussman L, Dobiner V, Sandbank J, Cagnano M, Cohen H, Sabo E: Ki67 antigen and PCNA proliferation markers predict survival in anorectal malignant melanoma. *Histopathology* 2002, 41:519–525
18. Zambrowicz BP, Friedrich GA, Buxton EC, Lilleberg SL, Person C, Sands AT: Disruption and sequence identification of 2,000 genes in mouse embryonic stem cells. *Nature* 1998, 392:608–611
19. Kim JY, Kang YS, Lee JW, Kim HJ, Ahn YH, Park H, Ko YG, Kim S: p38 is essential for the assembly and stability of macromolecular tRNA synthetase complex: implications for its physiological significance. *Proc Natl Acad Sci USA* 2002, 99:7912–7916
20. Harding HP, Novoa I, Zhang Y, Zeng H, Wek R, Schapira M, Ron D: Regulated translation initiation controls stress-induced gene expression in mammalian cells. *Mol Cell* 2000, 6:1099–1108
21. Todaro GJ, Green H: Quantitative studies of the growth of mouse embryo cells in culture and their development into established lines. *J Cell Biol* 1963, 17:299–313
22. Blasco MA, Lee HW, Hande MP, Samper E, Lansdorp PM, DePinho RA, Greider CW: Telomere shortening and tumor formation by mouse cells lacking telomerase RNA. *Cell* 1997, 91:25–34
23. Kim MJ, Park B-J, Kang Y-S, Kim HJ, Park J-H, Kang JW, Lee SW, Han JM, Lee H-W, Kim S: Downregulation of fuse-binding protein and c-myc by tRNA synthetase cofactor, p38, is required for lung differentiation. *Nat Genet* 2003, 34:330–336
24. Gallucci RM, Simeonova PP, Matheson JM, Kommineni C, Gurjel JL, Sugawara T, Luster MI: Impaired cutaneous wound healing in interleukin-6-deficient and immunosuppressed mice. *FASEB J* 2000, 14:2525–2531
25. Gallucci RM, Sloan DK, Heck JM, Murray AR, O'Dell SJ: Interleukin 6 indirectly induces keratinocyte migration. *J Invest Dermatol* 2004, 122:764–772